Signal feedthroughs for the ATLAS barrel and endcap calorimeters

D. Axen
Department of Physics, University of British Columbia, Vancouver, B.C., Canada

R. Hackenburg, A. Hoffman, S. Kane, D. Lissauer, D. Makowiecki, T. Muller, D. Pate, V. Radeka, D. Rahm, M. Rehak, S. Rescia, K. Sexton, and J. Sondericker
Brookhaven National Laboratory, Upton, NY

P. Birney, A.W. Dowling, M. Fincke-Keeler, T. Hodges, F. Holness, N. Honkanen, R. Keeler, R. Langstaff, M. Lenckowski, M. Lefebvre, P. Poffenberger, and G. Vowles*
Department of Physics and Astronomy, University of Victoria, Victoria, B.C., Canada

C. Oram
TRIUMF, Vancouver, B.C., Canada
(Dated: November 23, 2004)

The construction of the signal feedthroughs for the barrel and endcap ATLAS liquid argon calorimeters is described. The feedthroughs provide a high density and radiation hard method to extract signals from the cryogenic environment of the calorimeters using a novel design based on flexible kapton circuit board transmission lines.

PACS numbers: 29.40.V

I. INTRODUCTION

The physics reach of the ATLAS detector at the Large Hadron Collider (LHC) depends critically on calorimetry[1] to identify and measure the energy of leptons, photons and jets. In order to satisfy the required high granularity and resolution while operating in a high radiation environment, liquid argon based calorimetry[2] was chosen for the electromagnetic calorimeter of the barrel region[3] and for the electromagnetic and hadronic calorimeters of the endcap regions. The advantages of liquid argon calorimetry outweighed the difficulties associated with the necessity of cryostats and the consequent electrical feedthroughs to carry signal, monitoring, calibration and low voltage lines between the liquid argon (LAr) and the warm environment.

The feedthroughs have to satisfy several stringent mechanical and electrical requirements[2]. They provide 122 880 electrical connections in the barrel and 96 000 in the endcaps. They must preserve the insulating vacuum of the cryostat in a fail-safe way while being able to accommodate the relative movement of the warm and cold cryostat walls as the cryostat cools down or warms up. The mechanical components and welds must satisfy the pressure vessel laws of Europe where they are installed and North America where they were built. The feedthroughs must be highly compact and radiation resistant. Each electrical conductor should transmit less than 7 mW of heat in order to limit condensation problems that would affect the electrical signals. Calibration considerations demand that the resistance[4,5] of some of the lines be uniform to 0.5%. The cross talk between lines is required to be less than 0.8% between nearest neighbors and 0.2% in all other cases. Because of the large number of signal lines, and because of the required long lifetime of the cryostat, extreme constraints are imposed on the reliability of the feedthroughs and their signal lines. Tests of the electrical continuity after the feedthroughs were installed in the cyrostats showed there were zero failed channels.

In the ATLAS design, each feedthrough carries 1920 signal lines. The barrel cryostat has a total of 64 signal feedthroughs distributed radially in equal numbers around each end of the barrel. There is a total of 50 endcap signal feedthroughs also distributed radially in equal numbers around each endcap. High voltage for the calorimeters is supplied through separate high-voltage feedthroughs, which are not described here. The endcap feedthroughs also include a number of low-power supply lines for the pre-amplifiers in the endcap calorimeters (there are no pre-amplifiers in the barrel).

A novel aspect of the ATLAS signal feedthroughs is the use of flexible kapton circuit board transmission lines, henceforth referred to as vacuum cables. Very thin copper traces are laid down through photo-lithography to create highly uniform and reproducible striplines in a compact geometry. The transmission characteristics of the striplines are reasonably well-matched in impedance to the rest of the cable chain. Purpose-built connectors (pin carriers) with a very compact arrangement of pins designed to mate with the striplines are mounted in the warm and cold flanges. The pin carriers were designed to have excellent grounding connections that keep the cross-talk between neighboring signal lines low. Special care was taken to protect the signal and ground connections

*Present address: Department of Physics, University of Toronto, Toronto, Ontario, Canada.

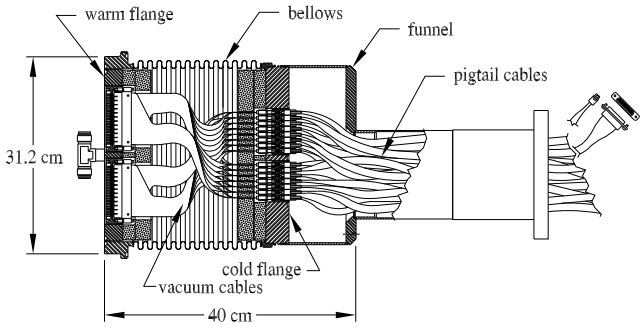

FIG. 1: An endcap signal feedthrough prior to installation.

from degrading with age.

In brief, the calorimeter cryostats consist of outer and inner warm vessels,where the inner vessel allows for an evacuated beam pipe to pass through the cryostat volume. Matching outer and inner cold vessels are located between the two warm vessels. Each feedthrough is welded to a transition piece (or pipe) on the outer cold vessel, and bolted to the outer warm vessel with a vacuum seal. The signal feedthroughs were assembled in close cooperation at two different sites, Brookhaven National Laboratory for the barrel feedthroughs and the University of Victoria for the endcap feedthroughs. The different geometries of the barrel and endcap create minor differences between the barrel and endcap signal feedthroughs. These differences will be pointed out when appropriate in the text.

Section II will discuss the mechanical construction of the feedthroughs and Section III the electrical aspects. The testing and quality assurance will be discussed in Sections IV and V.

II. MECHANICAL CONSTRUCTION

A. Overview

A sketch of a signal feedthrough is shown in Fig. 1. Mechanically, a feedthrough consists primarily of a warm flange, a cold flange, and a flexible bellows welded between the two flanges; this defines the volume of a feedthrough, as far as vacuum is concerned. The vacuum volume of a feedthrough is thus isolated from the insulating vacuum volume of the LAr calorimeter cryostat and in the case of the barrel, the vacuum for the liquid He solenoid that shares the same cryostat[2]. Pin carriers welded into the flanges provide the electrical connectors for the cabling in the three volumes (inner-cold, feedthrough-internal, and outer-warm). The bellows serves to permit a feedthrough to flex as the inner vessel is cooled to LAr temperature (87 K) and filled, while minimizing heat conduction and isolating the internal vacuum of the feedthrough. In the case of the barrel, the signal feedthroughs must accommodate a substantial relative shift in position between the warm and cold vessels when going from the warm, empty state of a calorimeter to the cold, filled state (and back). The geometry of the endcap cryostat results in a smaller shift between the warm and cold vessels during cool down.

The isolation of vacuum is important if minor leaks should develop in the pin carriers. An insulating sandwich of standard, cryogenic superinsulation is placed inside the bellows of the barrel feedthroughs, while layers of Rohacell (a polymethacrylimide hard foam) and aluminized mylar are placed inside the endcap feedthroughs. These function to restrict heat flow in the event of a leak, which would greatly increase heat flow through the feedthrough.

The liquid argon in the cryostats creates a maximum pressure difference of 2.8 bar on the barrel and 2.7 bar on the endcap cold flanges with vacuum on the other side (inside the bellows volume). Therefore pressure vessel codes apply. Table I shows the results of ASME[6] calculations for the minimum permitted thicknesses and the actual thicknesses used for the pressure bearing parts. The thicknesses used exceed the minimum required thicknesses by a comfortable margin.

Component	Minimum Required	Actual
Cold Box	0.66 mm	1.5 mm
Lower Tube	0.33 mm	1.9 mm
Flanges	11 mm	>12.4 mm

TABLE I: Comparison of minimum design thicknesses and actual thicknesses

B. Pin carriers

The pin carriers were manufactured by Glasseal[7], and consist of a stainless steel block with seven or eight rows of insulated pins. A schematic diagram of a 7-row pin carrier is shown in Fig. 2. Each pin carrier row (or slot) mates to one warm cable, vacuum cable, or pigtail cable. Identical pin carriers are used for the barrel and endcap feedthroughs and they are arranged in exactly the same manner on the warm and cold flanges.

Each flange has two 7-row and two 8-row pin carriers, for a total of eight pin carriers per feedthrough corresponding to thirty rows of pins on each of the warm and cold flanges. Vacuum cables, described in Section III B, connect the warm and cold flanges. Since a pin carrier row contains 64 pins in a standard, dual-in-line configuration, there are a total of 512 pins in the 8-row pin carriers and 448 for the 7-row, providing connections for 1920 signal lines per feedthrough.

The pin carriers employ glass as an economical insulating sealant around each pin. In order to match the expansion coefficient of the glass the metal required for the pins is softer than normally used for electrical pins

but is adequately hard for our needs. Although the softer pins were more easily bent, in most cases it was possible to straighten them again without breakage. The grounding connections are strictly through the pin carrier housings; this permits a greater economy of signal lines, i.e., no pins are devoted to carrying grounds. The pins are all gold-plated, as is the exposed inner metal surface of the pin carriers, to ensure good ground contact as well as good signal contact which should not degrade with age.

C. Warm and cold flanges and the seal ring

While the warm and cold flanges perform a simple function, viz., to hold the pin carriers and to define the insulating vacuum of a feedthrough, there are subtleties involved in their design. In particular, a maximum usage of the area is desired to keep the size and number of the feedthroughs as low as possible. This presents a difficult manufacturing problem by requiring the four pin carriers to be as close together on a flange as possible, while leaving enough room between the pin carriers for welding. Furthermore, the pin carriers are sensitive to stresses caused by the welding process as well as deflections under pressure during calorimeter operation. Therefore, the specifications call for a thick pin carrier body and a corresponding thickness for the flanges, exacerbating the problems caused by welding. In order to minimize the total heat input required for welding the material in the area to be welded was reduced. In this case, thin, close-tolerance weld preparations were machined on the pin carrier body and the flanges using standard end-mill tools. Close tolerances are required to promote a good fit, which is essential for reducing the heat input needed to achieve a good weld.

A further design-feature of the weld-preparation design on the flanges facilitates machining of the weld to remove any pin carrier which develops a leak after welding to a flange. This is an important economical consideration, because one leaking pin carrier would otherwise require three good pin carriers and a flange to be discarded. The height of the weld-preparation on the flange is designed to permit up to three such removals. Four pin carriers required such removal over the course of construction of the barrel and endcap feedthroughs.

There are small differences in the flanges used for the barrel and endcap feedthroughs. These differences involve slightly different weld-preparation designs required to accommodate the different welding processes, discussed below in Section II F.

The bellows is welded to a seal ring, which is subsequently welded to a warm flange. This simplifies the machining of the warm flange, which is similar to the cold flange, and facilitates attachment of the bellows.

Atmospheric pressure will exist on one side of the warm flange and vacuum on the other during normal operation. It is possible, in the event of a vacuum failure in the calorimeter, that the warm flange could be exposed to a pressure rise in the vacuum space of up to 3.2 bar for barrel feedthroughs and 3.1 bar for endcap feedthroughs[8]. Any significant deflection of the pin carrier in the region where the pins are located might result in the breakage of the glass bond. Finite element analyses of these exceptional situations were performed[9] to ensure that the resulting deflections and stresses are acceptable.

The bellows side of the cold flange is under vacuum and the other side (LAr side) is at a maximum pressure of 2.8 bar for barrel feedthroughs and 2.7 bar for endcap feedthroughs[8] during normal operation. Feedthroughs are required to be tested with a gas pressure of 3.5 bar for the barrel and 3.4 bar for the endcap, and this sets the most stressful conditions. Finite element analyses of this test condition were performed[9]. The maximum stress is found to be localized in the corner of the weld region of the pin carriers; 115 MPa is found for the endcap feedthroughs. The stresses in the sensitive region of the pin carriers were found to be low, below 10 MPa.

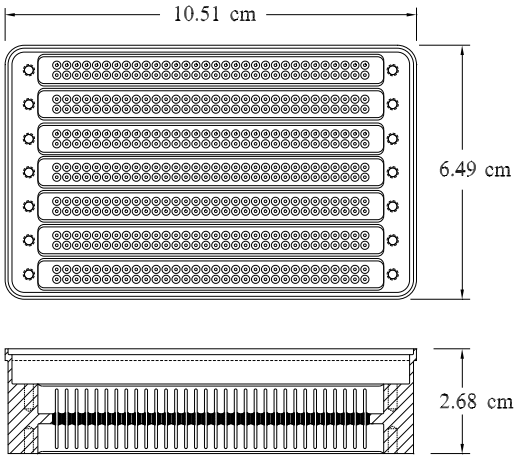

FIG. 2: A top and side view of a 7-row pin carrier.

D. Cold box and funnel assembly

At the bottom of a feedthrough, welded around the bottom of the cold flange, is the cold box, which provides room for the electrical connections to the pin carriers as well as room for the bend radii necessary for the pigtail cables. The cold box is fabricated from sheet stainless steel, and is rolled and welded with a single longitudinal seam. At the bottom of the cold box is the funnel tube, offset slightly from the center of the feedthrough to permit the barrel feedthroughs to be mounted slightly further out from the center of the barrel, to clear the hadronic (tile) calorimeter. This offset was also maintained in the design of the endcap feedthroughs. The feedthroughs are manufactured with a longer funnel tube than needed in order to facilitate leak testing; the excess length is cut off just prior to welding onto an aluminum-to-steel transition piece on the cryostat, as shown in

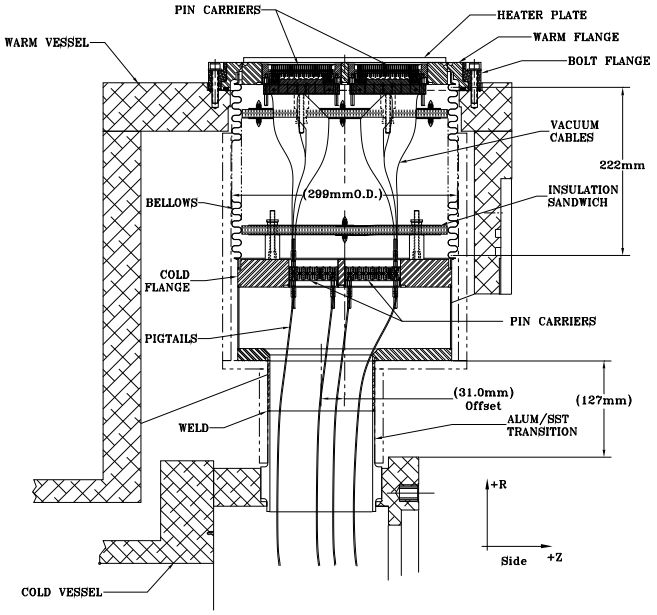

FIG. 3: A signal feedthrough installed on a barrel cryostat.

Fig. 3.

Finite element analyses of the cold box were performed[9] assuming the test gas pressure of 3.5 bar, and including a lateral force simulating the force required to displace the bellows laterally by 15 mm, this displacement occurring only for the barrel feedthroughs due to the contraction of the barrel cryostat on cooling to LAr temperature. All stresses were verified to be acceptable. In particular, the stress in the transition piece was found to be low, less than 6 MPa.

E. Bellows

The bellows are formed from 0.20 mm thick Type 316L austenitic stainless steel[2,10] with 14 convolutions in the barrel and 13 in the endcap. They conduct heat at a rate of less than 1 W per feedthrough[2,10]. The bellows is nominally 254 mm in diameter, with a 273.1 mm inside diameter and a 298.4 mm outside diameter. For the barrel feedthroughs, the bellows is welded on both ends to a cuff to facilitate subsequent welding into the signal feedthrough assembly. The cuff is machined from Type 304L austenitic stainless steel with a 279.4 mm inside diameter and 22.9 mm length, and having a 1.52 mm thickness at the ends for joining to the adjacent component. This yields an overall length of 259 mm for the relaxed length of the barrel bellows assembly. The endcap bellows have a cuff welded on the cold end, and an integrated cuff and seal ring welded on the warm end.

A free-standing bellows is essentially a big spring, with spring constants of 135.2 N/cm for axial motion and 285.1 N/cm for lateral motion. The change in position between warm and cold is calculated to be 12.7 mm in z toward the center of the cryostat while radially, the motion varies from 14 mm at the top to 10 mm at the sides to 6 mm at the bottom. The variation in the radial motion is due to the shift of the center of the cold vessel relative to the center of the warm vessel from warm to cold temperatures. This results in a total stress of 1.12 GPa in the deflected, cold state. As mentioned earlier, the lateral bellows motion for the endcaps is small.

The bellows is not subjected to either external or internal pressure during normal operation, since it has insulating vacuum on both sides. However, the possibility exists of a pin carrier developing a leak on the cold side, which would introduce argon into the bellows volume[11]. Failure of a pin carrier in a cold flange located at the bottom of the cryostat determines the worst case scenario requiring a specified test pressure of 3.5 bar. The calculated critical pressure P_{cr}, or squirm pressure [a], is 2.8 bar using the Expansion Joint Manufacturers method[12], or 3.7 bar using the CODAP[13] method. The actual P_{cr} was evaluated by testing. The manufacturer[14]tested a representative bellows by welding restraints inside the bellows assembly and then pressurizing. Their test resulted in some expansion at 2.1 bar. Onset of squirm occurred between 4.0 bar to 4.1 bar. Tests at the Brookhaven National Laboratory using water pressure showed the onset of squirm in an initially relaxed bellows at 4.3 bar. The bellows, although distorted, reach an ultimate pressure of 11.7 bar. A test conducted with a bellows offset 13 mm laterally, while the axial length was maintained showed the onset of squirm occurred at 4.0 bar.

Section 8.5.2.4a of the CODAP[13] requires that bellows that are offset must have a P_{cr} which is 10 times greater than the designed operating pressure. Using this criterion, the signal feedthrough bellows design operating pressure is downgraded to 0.4 bar, and the maximum pressure in the vacuum space must be limited to less than this derated pressure. Hence, a relief valve is installed on each feedthrough to prevent the pressure from rising above 0.4 bar in the event of a catastrophic leak.

F. Welds

The signal feedthrough cross-section is shown in Fig. 4, where the left half corresponds to an endcap feedthrough and the right half a barrel feedthrough. Weld types differed in some cases between the barrel and endcap feedthroughs in order to match the welding equipment and expertise at each of the two assembly sites. Where the weld types differ, they are prefixed by 'E' for endcap or 'B' for barrel in the enlargements of the weld joints shown in Fig. 4. The mechanical and weld design of the ATLAS signal feedthroughs conforms to the Ameri-

[a] Squirm is defined as the onset of nonlinearity in the bellows' expansion as a function of pressure.

can Society of Mechanical Engineers (ASME) Boiler and Pressure Vessel Code[6] and the CERN Safety Code D2, Pressure Equipment[15]. During fabrication, the stricter inspection requirements of the French CODAP[13] and CERN[15]were also observed.

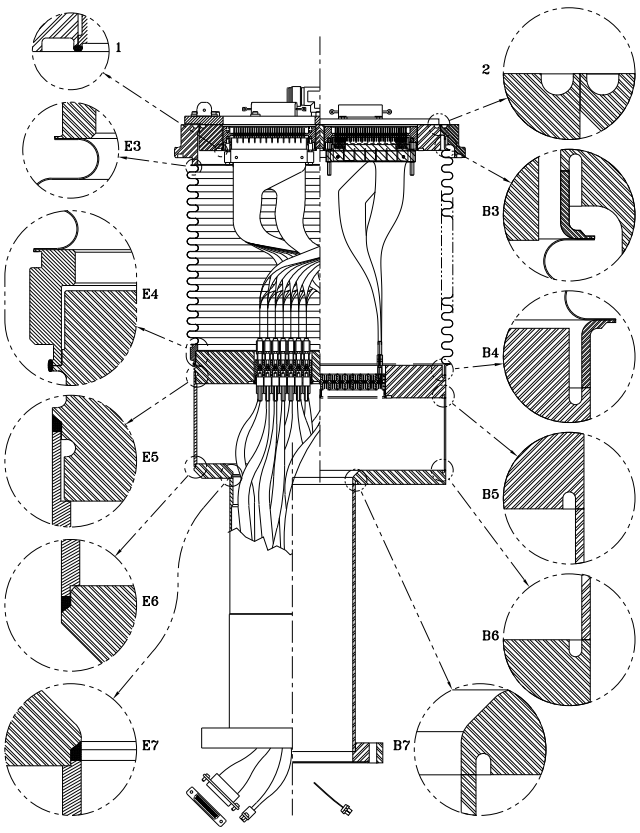

FIG. 4: The welds on a signal feedthrough; the barrel (endcap) specific welds prefixed with a 'B' ('E').

For the barrel feedthroughs, an autogenous Gas Tungsten Arc Welding (GTAW) process was selected to permit precise control of the fuse zone and, therefore, the heat input. The circumferential welds were designed to be accomplished in a single pass by a hand-held welding torch with the weld-pieces tack-welded together and held in place on a variable speed turntable. For the endcap feedthroughs, a two pass weld was used for the three cold box welds (E5, E6, E7). The first pass was an autogenous weld to ensure root penetration. With the second pass, filler material was added to complete the weld. These welds were done manually on a hand-rotated turntable.

Weld joint 1 is the connection of the pin carriers to the warm and cold flanges. It is performed using an edge weld. Research at Brookhaven National Laboratory for the Relativistic Heavy Ion Collider found that edge welds typically have only as much penetration as the thinnest section being fused[16]. Therefore the weld procedure must be validated. For this purpose, a separate weld procedure was developed and qualified specifically for the pin carrier edge welds at both assembly sites. A production pin carrier and flange were welded, after which a section was cut from each of the four sides for micrographic inspection. These micrographs are shown in Fig. 5. A pressure test also was conducted, where a production pin carrier was welded into a specially machined Conflat© blank flange. The specimen was bolted to another blank flange with a tube welded into the center for fluid access, and pressurized with water. The Conflat© flange began leaking at 58.6 bar. Pressure was reduced to 51.7 bar and held for 10 minutes. The pin carrier was then leak checked to 10^{-5} mbar-l/s with no leaks detected.

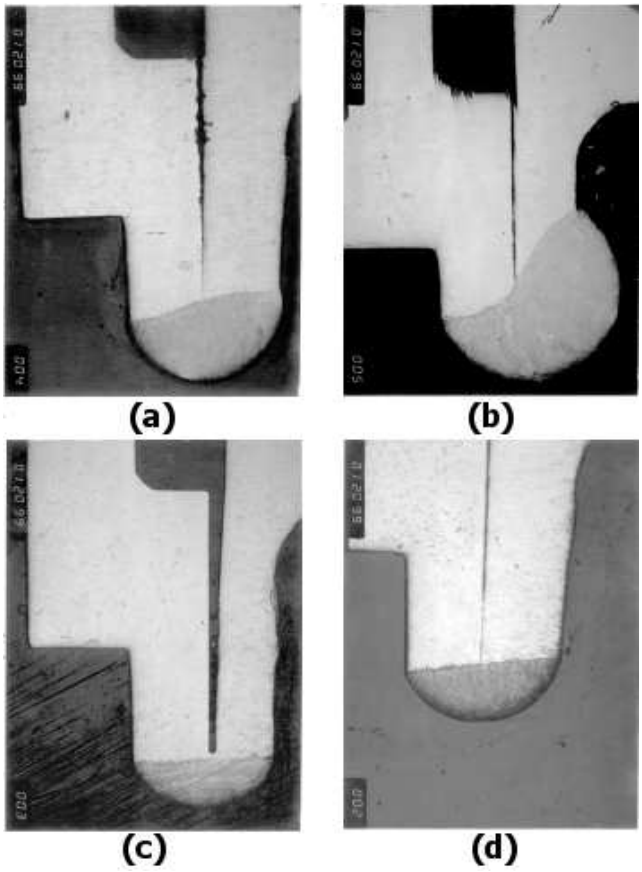

FIG. 5: Pin carrier weld qualification micrographs, 32× magnification. The micrographs shown are: (a) exterior longside; (b) exterior shortside; (c) interior shortside; (d) interior longside.

Weld joint 2 is the connection of the warm flange to the seal ring. It is subjected to atmospheric pressure from the outside when the vacuum space of the signal feedthrough is evacuated, and the joint is subjected to the spring forces created by the deflection of the bellows. This type of joint is a commonly used vacuum technique. The lips created by the grooves machined into the adjacent material are autogenously fused together.

For the barrel feedthroughs, weld joints B3 and B4 are square butt welds used to join the bellows to the seal ring and cold flange. The thin sections are machined to match the thicknesses of the bellows assembly cuffs. Weld B3

can be visually inspected from both sides. Weld B4, however, which is done after the cables have been installed, closes the volume and so eliminates the possibility for inspection on the inside. The cold flange meets the bellows assembly at a point lower than the surface of the cold flange to greatly reduce the risk of hot material getting inside the vacuum volume during welding. This was verified by positioning a layer of kapton within 13 mm of the joint on the inside of the vacuum volume during qualification testing, simulating the presence of vacuum cables. No damage was found on the kapton after welding. Machined surfaces on both sides of the joint provide the very close fit necessary for a good square butt weld. For the endcap weld E4, the bellows cuff ring was sealed to the cold flange with an edge weld.

Weld E5/B5 is the upper attachment of the cold box to the cold flange. For the barrel feedthroughs, its configuration is identical to weld B4. The cut to fabricate the sheet produces a sufficiently precise fit for welds B5 and B6 with only minor finishing at the ends of the longitudinal weld. Weld B5 is performed after the pin carriers are installed in the cold flange, but before any cables are connected. This permits inspection of the weld on both sides. Weld E5 was performed on the endcap feedthroughs after all electrical cables were installed.

Weld E6/B6 is the lower attachment of the cold box to the funnel flange. For the barrel feedthroughs, its configuration is identical to welds B4 and B5. The thin section on the funnel flange is machined to match the thicknesses of the cold box. Weld B6 is performed after the pigtail cables are connected and tested, eliminating the ability to further inspect the inside of the cold box. For the endcap feedthroughs, welds E6 and E7 were performed in advance during fabrication of the cold box assembly.

Weld E7/B7 is the attachment of the lower tube to the funnel flange. This is the thickest section welded on the entire device. The lower tube is fabricated from standard (stainless steel) Schedule 5 pipe, which has a thickness of 2.8 mm which is within the capacity of a single-pass GTAW joint. For the barrel feedthroughs, the thin section on the funnel flange is machined to match the thicknesses of the lower tube. This weld is performed first for the cold box volume, permitting inspection from both sides. Standard ASME qualification testing, consisting of root and face bend tests, were performed using Schedule 5 pipe from part of the lot procured for production. [b]

A separate qualification procedure was prepared specifically for CERN. The cold volume of the signal feedthrough was subjected to a pressure test. Test specimens were prepared at both BNL and Victoria using production components. Flat plates were welded over the holes for the pin carriers in the cold flange for the test specimen. The test specimen included the Conflat© flange at the bottom of the lower tube. This flange is not used in the experiment, but is used to facilitate production testing, including fabrication pressure testing. This flange was capped using a blank Conflat© flange drilled and tapped to accept standard pressure fittings for a hydrostatic test. The lower tube started to deflect at 34.5 bar, due to the eccentric location within the flange. Testing was stopped at 66.9 bar, when the Conflat© flange began leaking. While the lower tube had deflected significantly, due to flange distortion, no joint had failed or yielded. The cold box also bulged slightly, which was expected since it was only designed for 2.8 bar.

The ASME[6] inspection requirements depend on the safety factors used in the design, and include visual inspection of each weld and a pressure test to 125% (pneumatic, as opposed to 150% hydrostatic) for the pressure-bearing welds when more conservative safety factors are used in the design, as in this case. The CODAP[13] also would have allowed these less stringent and less costly requirements in their Construction Category C. However, CERN imposed the more conservative Construction Category A for inspection, and mandated radiographic inspection where practicable. Welds B5 and B7, as well as the longitudinal welds of the cold box and lower tube were radiographically inspected. Dye-penetrant inspection was employed for weld B6 because the inside volume was not accessible. For the endcap feedthroughs, the longitudinal weld of the cold box was radiographically inspected, while the welds E5, E6, and E7 were dye-penetrant tested.

G. Vacuum

The feedthroughs are pumped by a system separate from the one providing the high vacuum for the insulating volume between the inner and outer cryostat vessels. The feedthroughs are constructed with two, switchable vacuum ports welded into the warm flange, providing for the possibility of a dual vacuum system. The dual vacuum system permits separate pumping on any feedthrough which may develop leaks during the course of its life, without compromising the vacuum in the other feedthroughs. Tests at Victoria showed that a pressure of less than $\sim 10^{-1}$ millibar is adequate for the feedthrough vacuum in order to maintain good heat insulation. Thus, some small number of leaking feedthroughs would not deprive ATLAS of a calorimeter during a physics run. Control-line pressure-activated valves on each feedthrough select one of the two vacuum pumping systems; the positions of the valves are sensed from double-position micro-switches on each valve.

[b] Root and bend tests consist of cutting longitudinal strips from the pipe across the weld, then bending the strips once at the weld into a "vee" shape, some with the exterior, welded side facing outside the bend, and some with the interior, welded side facing outside the bend, the latter exposing the "root" of the weld.

H. Heaters

Heat conduction primarily through the vacuum cables cools the warm flange and pin carriers and therefore condensation and frosting could occur on the outer face of the warm flange and pin carriers[23]. To prevent this, heater plates are installed on the outer face of the warm flanges. The barrel feedthroughs employ a commercial design[24] involving a heater element not unlike that found in household kitchen range-tops. As a redundancy, the heaters consist of two independent halves. Each half has a resistance of 25 Ω and is rated at a maximum of 50 volts (i.e., 2 A), but is expected to operate at a fraction of that, unless a serious leak develops in a feedthrough. For the endcap feedthroughs, the heaters are based on a design using six 75 Ω resistors wired in parallel (12.5 Ω equivalent) and arranged on the outside perimeter of an aluminum heater plate. The resistors each have a power rating of 50 W. A pad of thermally conductive graphite tape is placed beneath each resistor to improve heat conduction to the heater plate, and a 0.025 inch thick pad of thermally conductive silicone rubber sheet is placed between the heater plate and warm flange to improve heat conduction to the flange. Each of the resistors is individually fused, so that the failure of any one of the six resistors will not impact the operation of the others. This design provides a high level of redundancy should any of the resistors fail. Samples of resistors were subjected to a number of tests in order to qualify their reliability. For some of the tests, the resistors were 50 Ω rather than 75 Ω, but of the same type and from the same manufacturer. The tests included:

- Resistors were mounted to a water-cooled base and powered at 50 W, their specified power rating, for a period of 286 days. The resistors' surface temperature was about 65° C for this test.
- Resistors were powered at 5.1 W for a period of 308 days, not water cooled, with a surface temperature of 100° C.
- Resistors were subjected over a period of 52 days to 4700 cycles of being dunked in water, then powered at 5.4 W with a surface temperature of about 50° C.
- Resistors were subjected over a period of 36 days to 1080 cycles of being dunked in water, then powered at 1.3 W with a surface temperature of about 40° C. The resistors under test would be placed wet in a freezer each evening for the duration of this test.

No resistors failed after any of these tests.

For each barrel and endcap heater, 50 W supplies are provided for normal operation, which, together with ambient heating, are more than adequate. During cold tests of the completed ATLAS barrel detectors and cryostat system, it was found that 15 W was sufficient to maintain the feedthrough warm flanges at a temperature of 20° C, consistent with expectation. A 150 W supply will be connected to any heater which sits on a leaking feedthrough, if one occurs, to keep the frost off despite a substantial heat leak. The power leads installed on all of the heaters are designed to accommodate this larger current. Two thermocouples mounted on the warm flange are used to regulate the power fed to the heaters.

III. ELECTRICAL CONSTRUCTION

A. Overview

A feedthrough electrically connects the pin carriers in the warm flange to those in the cold flange by 30 vacuum cables. Four of the signal feedthroughs for each endcap have special vacuum cables for the purpose of delivering low voltage power to the pre-amplifiers in the endcap hadronic calorimeters, otherwise all signal vacuum cables are identical with a resistance about 0.95 Ω and a characteristic impedance of about 33 Ω. From the bottom of the cold flange, outside the bellows volume, are connected 30 coaxial cables of ten different types, referred to as pigtail cables. Once ATLAS is in operation, the pigtail cables will be immersed in LAr. Connecting the top of the warm flange to the electronics crates are 30 cables, referred to as warm cables. A complete description of the cabling for the ATLAS calorimeters and signal feedthroughs can be found elsewhere[17,18].

Grounding connections were problematic during the prototyping phase; this was determined to be due to a lack of gold-plating on the prototype components, and a weak spring-leaf construction in the prototype cables. This was solved by gold-plating all of the electrically connecting surfaces and by employing stiffer spring-leaves on the cable connectors.

B. Vacuum cables

The vacuum cables are flat, polyimide stripline flexible cables[2] and are designed to flex with the bellows during filling and emptying of the cryostat. A photograph of a signal vacuum cable is shown in Fig. 6. The large number of readout channels in the ATLAS LAr calorimeters contributes a significant heat leakage into the cryostats and requires a careful consideration of the kind of conductors to use. Microstrip transmission lines were chosen in order to minimize heat conduction while maintaining signal integrity. It is estimated that the total heat loss[2] through a feedthrough due to the vacuum cables is about 18.7 W, with a total of about 19.7 W including the heat loss through the bellows. These cables must be very reliable since they are contained in a welded-shut volume, inside the bellows and between the warm and cold flanges. The vacuum cables are therefore subjected to extensive testing[5], described below in Section V, before and after this volume is welded shut. There are two striplines per vacuum cable, with 32 transmission lines per stripline.

FIG. 6: A signal feedthrough vacuum cable. Two polyimide flexible striplines each with 32 transmission lines lie one atop the other. The connectors at each end are 2×32 sockets to mate with the pin carriers.

Each transmission line consists of a copper signal trace and a copper ground trace separated by 51 μm of polyimide dielectric[c]. The nominal widths of the signal and ground traces are 204 μm and 357 μm, while the nominal thickness is 34 μm for each. The manufacturer[19], however, was allowed to make minor adjustments to these dimensions in order to meet the impedance and resistance requirements. Both signal and ground traces are covered with 76 μm of polyimide and adhesive[d]. The two striplines of each vacuum cable are arranged such that the signal traces face each other on the inside and the ground traces are facing the outside. A theoretical model of the vacuum cable transmission line is presented in Appendix A.

The connectors at each end of the vacuum cable have 64 gold-plated sockets arranged in a 2×32 configuration in order to mate the 64 signal traces to the 64 pins of a pin carrier slot in the cold and warm flanges. The ground traces are connected to the pin carrier by gold-plated ground shields on either side of each connector. The 32 ground traces of each stripline are common to the connector ground shields on the corresponding side of the connector, however the grounds on each side of the connector, and hence of the two striplines, are isolated from each other.

C. Pigtail cables

Three different types of pigtail cable[20] are used for the barrel: 50 Ω, 75 cm long; 50 Ω, 50 cm long; and 25 Ω, 50 cm long. Seven different types of pigtails are used in the endcap feedthroughs: 25 Ω and 50 Ω, 90 cm long cables for the electromagnetic calorimeters, presampler, and some monitoring channels; 25 Ω, 430 cm long cables for the forward calorimeters; and three types of 50 Ω, 265 cm long cables for the hadronic calorimeter signals plus one type of 265 cm long cable for the hadronic calorimeter low voltage preamplifier power supplies.

Each pigtail cable consists of a bundle of 64 polyimide-wrapped coaxial cables, with the exception of the pigtails for the low voltage power supplies which have only 60 cables per bundle. The diameter of each individual coaxial cable is about 1.05 mm for the 25 Ω cables, 1.11 mm for the 50 Ω cables, and 1.19 mm for the low voltage power supply cables. The pigtail cables connect to the cold flange with a 2×32 connector similar to that used for the vacuum cables. For most of the pigtail cables, the connector at the other end is a high density 100-pin μD, with 64 pins connected to signal wires and 34 to ground. The signal and low voltage supply pigtail cables for the hadronic calorimeter use different connectors, with eight 2×8 pin connectors for each of the signal cables and ten 2×8 pin connectors for each low voltage supply cable. The pigtail connectors attach to patch panels inside the active volume of the calorimeter, in LAr, which are connected to the calorimeter elements and calibration/monitoring circuits. The pigtail cables were manufactured by Axon'[21] in close cooperation with LAL Orsay. The pigtail cables were subjected to rigorous testing by the manufacturer, plus additional testing, described below in Section V, at the feedthrough assembly sites prior to installation into the feedthroughs.

D. Warm cables

Electronics crates sit on top of pairs of feedthroughs, except for one crate on each endcap which has only one feedthrough; each feedthrough connects to half of a crate's backplane. The feedthroughs are connected to the electronics crates with warm cables, of a very similar design to the vacuum cables except they are shorter, 28.5 cm long face-to-face, and have a different connector on the end which connects to the backplane of the electronics crate. In addition, there are a few special 33.5 cm long warm cables on the endcaps as well as PEEK insulated AWG22 gauge wires, to carry low voltage to supply the pre-amps in the endcaps. The 33.5 cm long signal cables are necessary due to a longer than normal distance from the pin carrier slot to the baseplane slot for some positions. In principle, the warm cables are replaceable but since access to the experimental hall is very limited, they are subject to the same, stringent testing applied to the vacuum cables.

[c] DuPont AP9121 Copper-Clad Laminate
[d] DuPont LF0120 Pyralux LF Coverlay

E. Low voltage cables

The pre-amplifiers for the hadronic endcap (HEC) signal readout are located inside the LAr cryostat. The low voltage (LV) supplies for those preamplifier boards pass through the signal feedthroughs. Since the microstriplines, which carry the signal pulses, are too thin to accommodate the currents of the HEC preamplifier LV lines, special cables were devised to carry the maximum foreseen currents while keeping the heat transfer to a minimum[22]. There are four such LV cables in each of the four HEC signal feedthroughs on each endcap cryostat. The preamplifier boards do not all consume the same power, so LV vacuum cables with a combination of three different gauge wires (AWG24, AWG26, and AWG28) were chosen so that each wire can carry its anticipated current load, with a sufficient safety margin, while minimizing the heat-conducting copper cross section. Heat loss through the corresponding LV warm cables is not such an issue, so those wires are all AWG22 gauge. All low voltage vacuum cables were subjected to rigorous testing before installation.

F. Sensor and control connections

In addition to the signal, calibration, and monitoring lines carried by the signal feedthroughs, there are several external control and monitoring lines, which do not enter the cryostat. Because these control lines are brought in from the outside to the vicinity of the readout electronics, they are potential sources of noise and ground-loops. To prevent such problems, strict ground-isolation was implemented, and these lines were all brought in through a filter box[23], with one box shared by each pair of feedthroughs. The same filter boxes are used on the barrel and endcap calorimeters. Each filter box handles four thermocouples, four vacuum switch position sensors, and two heater currents.

IV. LEAK TESTING AND COLD-CYCLING

All of the individual mechanical components were separately leak tested with a commercial helium-based leak detector prior to assembly, to reduce expenses arising from assembling defective pieces. Test benches were constructed at each feedthrough assembly site, with ports for each type of component, and switching valves to select the port in-use. Additionally, any assembly, including the pin carriers, were thrice cold-cycled with liquid nitrogen (LN_2, 77 K) and then leak-tested again to ensure that no leaks would develop from cold-cycling. Because the cold-cycling tests were not intended to be cold-shock tests, automated devices were designed to limit the temperature gradient during cool down of the pin carriers. For the barrel feedthroughs, a lowering apparatus was constructed to lower a basket of components slowly into a dewar of LN_2, maintaining a small space above the surface of the liquid until the components were sufficiently chilled to be lowered all the way into the LN_2. For the endcap feedthroughs, a cryogenic refrigerator was used to cool the pin carriers to a temperature of 77 K over a period of 20 hours.

For the purpose of cold-testing each feedthrough in a realistic scenario, where all the requisite vacuum and pressure volume tests could be performed simultaneously with the electrical tests, simulated cryostats were constructed at both assembly sites that could accommodate a feedthrough mounted to it without welding. Each feedthrough was in turn mounted on the test vessel and cooled to LN_2 temperature by filling the vessel with LN_2, and the bellows evacuated. Extensive leak and pressure tests were then performed, followed by a full battery of electrical tests, described in more detail in Section V. Following warm up, the cold volume of each feedthrough was again pneumatically pressure-tested and all electrical tests repeated. Two barrel and four endcap feedthroughs developed shorts between one pair of signal lines in the vacuum cables during the cold tests. These six feedthroughs were opened up, had the defective vacuum cables replaced, and then closed again. In the case of the two barrel feedthroughs, this operation also necessitated the replacement of the bellows. All tests were successfully repeated on the repaired feedthroughs. The problem with the vacuum cables in those feedthroughs was later determined to be excessively large solder beads on neighboring pairs of signal lines which made contact with each other only when cold.

V. ELECTRICAL TESTING DURING ASSEMBLY

For the barrel feedthroughs, two types of test were performed on every signal line in every cable used in the feedthroughs, i.e., the warm cables, the vacuum cables, and the pigtails. The first test was an automated continuity test, which checked every line for continuity and also for leakage into other lines. The continuity test also checked the ground connections; because of the requirement that the ground connections be very low resistance, the ground continuity was checked with a four-wire method.

The second test was a time-domain-reflectometry (TDR) measurement of each signal line[25]. The TDR waveform was digitized and analyzed for length and compliance with standard reference waveforms. Software determined whether each waveform, from each signal line, was a pass or fail, and recorded the waveform on a disk file. A commercial TDR device coupled through a switching matrix sequentially selected and tested each of the 64 lines in a cable. These tests were performed at every stage of assembly for the barrel feedthroughs, including:

1. Initial acceptance tests of incoming cables.

2. Pre-welding tests, when the cables in a feedthrough were all connected, but the bellows and cold box volumes had not yet been welded shut.

3. Post-welding tests, right after the bellows and cold box volumes were welded shut.

4. Final, cold test, in which each feedthrough was mounted on a test fixture, which simulated the barrel cryostat, and was brought down to LN_2 temperature.

5. Final, warm test, after a feedthrough had warmed up after the cold test.

6. Pre-installation test, after a feedthrough had arrived at CERN, just prior to welding to the cryostat (TDR only).

7. Post-installation test, after a feedthrough had been welded to the cryostat (TDR only).

8. Post-warm-cable-installation test, after the warm cables had been connected between the backplane and a feedthrough (TDR only).

Some cables in the endcap feedthroughs will carry calibration signals. The spread in resistance among all channels of the calibration cables in a particular feedthrough is required to fall within a 50 mΩ band in order to maintain relatively uniform attenuation. The specification for trace resistance of the vacuum cables not used for calibration is not particularly stringent, $0.6\ \Omega < R < 1.2\ \Omega$. Both the absolute magnitude and spread in resistance is dominated by the vacuum cables when compared with the pigtail cables. The vacuum cables for the endcap feedthroughs were therefore passed through a number of tests, in part to select sets of cables which could be used for calibration.

The resistance of each signal trace of each vacuum cable was measured using a four-wire measuring technique for high precision, allowing the identification of those cables which could be used in the calibration slots. Fig. 7 shows a histogram of measured resistance from a sample of 574 vacuum cables of the endcap feedthroughs. The full width of this distribution is more than 300 mΩ, however there was no difficulty in finding a sufficient number of sets of cables whose resistances fell within the 50 mΩ band required. Four additional tests were conducted on the vacuum cables to be used in the endcap feedthroughs. A cross talk test was conducted, where each individual channel is pulsed and then the pulsed channel and its nearest neighbors are read out. This test allows the identification of discontinuities in the ground traces, since the cross talk is significantly enhanced if the ground trace path is broken. The mean of the distribution of cross talk measured between adjacent nearest neighbors (i.e., nearest neighbor on the same stripline) is 0.23%, while the mean cross talk for opposite nearest neighbors (i.e., cross talk with the nearest signal line on the opposite stripline) is 0.69%. The cross talk in the latter case is higher due to

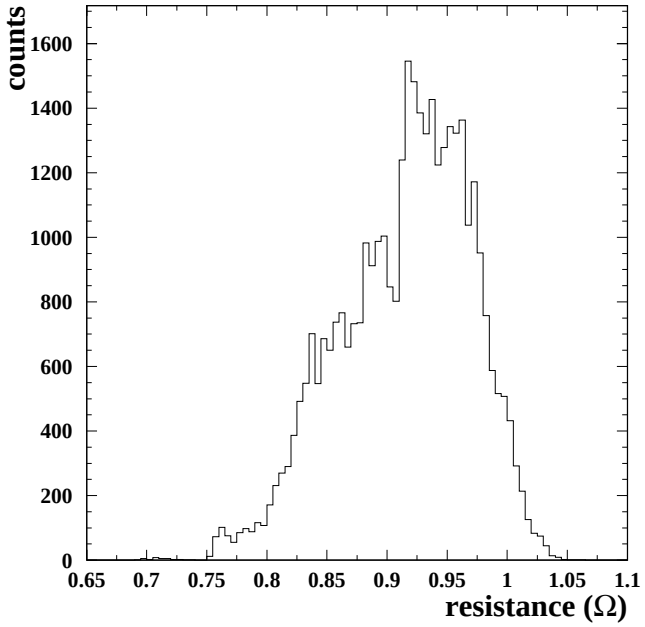

FIG. 7: Distribution of vacuum cable channel resistance from a sample of 574 endcap feedthrough vacuum cables

the capacitive coupling between the signal strips which lie against each other. The impedance of six representative strip-lines was also measured for each vacuum cable, and resistance measurements were made in order to verify good electrical contact between the ground shields of a vacuum cable and a pin carrier, and also between a ground shield on one end of a vacuum cable with the ground shield on the opposite end. Resistance between the pin carrier and ground shield was typically about 17 mΩ. Finally, a commercial cable tester was used to check continuity of the signal lines while the cables were gently wiggled. This test allowed the identification of vacuum cables with intermittent discontinuities in the signal traces.

Electrical tests were also conducted on the endcap feedthroughs during the assembly stage. An automated continuity test was performed during:

1. Pigtail assembly, when the pigtail cables were being connected to the cold flange.

2. Vacuum cable assembly, when the vacuum cables were being connected between the warm and cold flanges.

3. Pre-welding tests, when the cables in a feedthrough were all connected, but the bellows and cold box volumes had not yet been welded shut.

4. While the feedthrough was cooled to LN_2 temperature.

A cross talk test was also performed on the endcap feedthroughs during the following assembly steps:

1. While the feedthrough was cooled to LN_2 temperature.
2. Final warm test before shipping to CERN.
3. Pre-installation test, after a feedthrough had arrived at CERN, but prior to welding to the cryostat.
4. Post-warm-cable-installation test, after the warm cables had been connected between the backplane and a feedthrough.

In addition, a precision resistance test was performed for the endcap feedthroughs as part of the final warm test before shipment to CERN.

Although a few electrical channels required minor repairs after installation of the warm cables on the installed barrel and endcap feedthroughs at CERN, no failures were found in the combined 218 880 channels of the barrel and endcap feedthroughs once installation was completed.

VI. DATABASE

For the purposes of tracking problems and providing electrical test data to analysis code (should it ever prove useful to do so), the details of construction (i.e., serial numbers of components, etc.) and all test results were entered into databases, separate for the barrel and endcap. The barrel signal feedthrough database, except for the TDR tests, has been exported to the ATLAS Production Database[26] and a similar database for the endcap signal feedthroughs is in preparation.

VII. ACKNOWLEDGMENTS

We would like to thank Todd Corwin, John Meade, and Jason Farrell of BNL, as well as Alisa S. Dowling, John Lindner, and Wendy Wiggins of the University of Victoria, without whom these feedthroughs would never have been produced and installed. We would also like to thank LAL Orsay for the production and testing of the pigtails, and Aboud Fallou, Jacques Dubois, and Manuel Alves of LAL Orsay, Victor Zhabitskiy of IHEP, Russia, and Jean-Pierre Brachet, Jacques Fattaz, Gilles Favre, Werner Kubischta, Didier Lombard, Pascal Mesenge, and Giovanna Vandoni of CERN who provided assistance in the installation of the feedthroughs. Finally, we wish to acknowledge the invaluable assistance throughout the planning, construction, and integration stages provided by Martin Aleksa, Patrick Fassnacht, Allain Gonidec, and Pierre Pailler of CERN. This work has been supported by the Natural Science and Research Council of Canada, the Institut National de Physique Nucléaire et de Physique des Particules of France, the United States National Science Foundation under Cooperative Agreement PHY-9722537, and the United States Department of Energy under Contract No. DE-AC02-98CH10886.

APPENDIX A: FREQUENCY DEPENDENT MEASUREMENTS AND MODELING OF THE VACUUM CABLES

A typical ATLAS LAr pulse has a rise time of approximately 20 ns, corresponding to a bandwidth of 17.5 MHz. Frequency dependent measurements up to 50 MHz of the characteristic parameters of a vacuum cable are therefore adequate to describe its performance in ATLAS.

1. Measurements

In order to study the frequency dependent behavior of a vacuum cable, the complex impedance of the stripline has been measured with a network analyzer [e] in terms of its magnitude $|Z|$ and phase ϕ. This measurement has been performed with both open circuit ($|Z_{oc}|, \phi_{oc}$) and short circuit ($|Z_{sc}|, \phi_{sc}$) termination of the stripline [f]. Given the magnitude and phase, the complex quantities Z_{sc} and Z_{oc} can be constructed. Using the high frequency TEM mode approximation, it is possible to calculate characteristic stripline parameters from these measurements[27].

The characteristic impedance Z_o and the quantity $\tanh(\gamma l)$ are given by

$$Z_o = \sqrt{Z_{sc} Z_{oc}}\,, \tag{A1}$$

$$\tanh(\gamma l) = \sqrt{Z_{sc}/Z_{oc}}\,, \tag{A2}$$

where l is the length of the stripline and γ is the propagation coefficient $\gamma = \alpha + i\beta$, where α is the attenuation coefficient and β the phase-change coefficient of the cable. For a typical vacuum cable, the measured characteristic impedance as a function of frequency (up to 50 MHz) is shown in Fig. 8. For an electrical length of the stripline of 41 cm (including the connectors and terminator), the measured frequency dependence of the attenuation is shown in Fig. 9.

Based on the measured quantities, the resistance, inductance, conductance and capacitance (per unit length) of the stripline can also be determined:

$$R = \Re e(\gamma\sqrt{Z_{sc} Z_{oc}})\,, \tag{A3}$$

$$L = \Im m(\gamma\sqrt{Z_{sc} Z_{oc}})/2\pi\nu\,, \tag{A4}$$

$$G = \Re e(\gamma/\sqrt{Z_{sc} Z_{oc}})\,, \tag{A5}$$

$$C = \Im m(\gamma/\sqrt{Z_{sc} Z_{oc}})/2\pi\nu\,. \tag{A6}$$

[e] Network analyzer hp8735B in combination with with a hp85047A S-Parameter set.

[f] These measurements were performed on a preproduction cable. The impedance of the preproduction batch was slightly higher than the impedance of the final production.

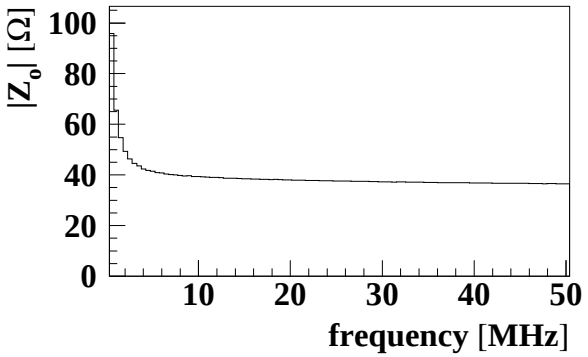

FIG. 8: Characteristic impedance measured as a function of frequency.

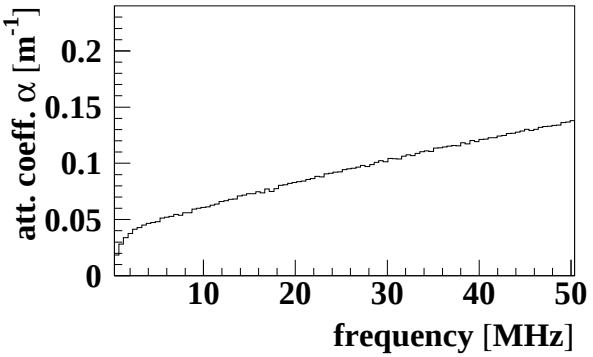

FIG. 9: Attenuation coefficient measured as a function of frequency.

The frequency ν dependence (up to 50 MHz) of these parameters is shown in Fig. 10.

These parameters allow a calculation of the phase velocity,

$$v_p = \frac{1}{\sqrt{LC}} = \frac{1}{\sqrt{\mu\epsilon}} \ . \qquad \text{(A7)}$$

Since the permeability of copper is $\mu_r \approx 1$, the phase velocity depends entirely on the relative dielectric constant ϵ_r. Using the values of L and C calculated from the measurements, v_p and ϵ_r can be determined. Their frequency dependence is shown in Figures 11 and 12. At a phase velocity of 0.16 m/ns, the propagation delay of a 40 cm long stripline is 2.5 ns, which is in good agreement with the time domain reflectometry (TDR) measurements made for the vacuum cables.

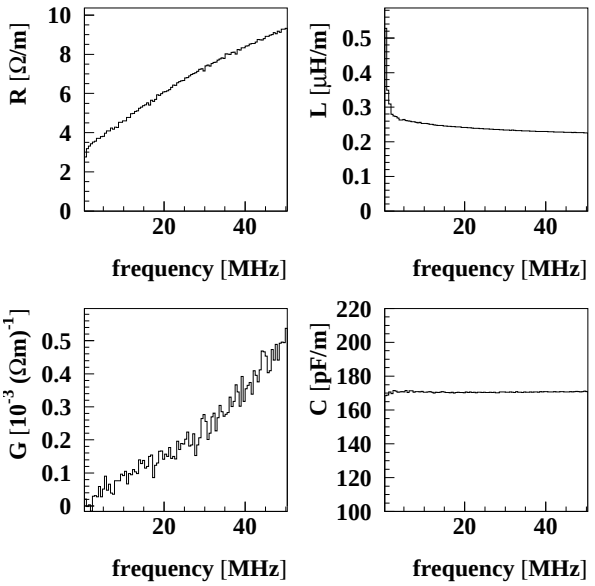

FIG. 10: Resistance, inductance, conductance and capacitance per unit length as a function of frequency, determined from measurements.

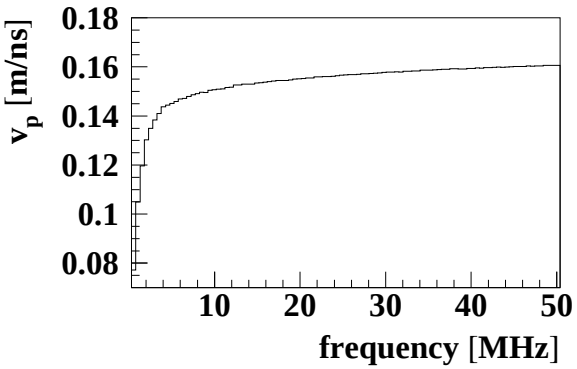

FIG. 11: Phase velocity as a function of frequency.

2. Theoretical Description of the stripline

Laplace's equation was solved numerically to obtain the electric field for a given conductor geometry. Applying Gauss' law then yields the capacitance per unit length. This technique allows a study of the effects of the variation of the stripline geometry and the effects of possible variations of the values of the material properties. Such variations can arise from the production process, which limits the accuracy on the width of the strips to about ± 10 μm. The relative dielectric constant ϵ_r varies with frequency, temperature, and humidity; for

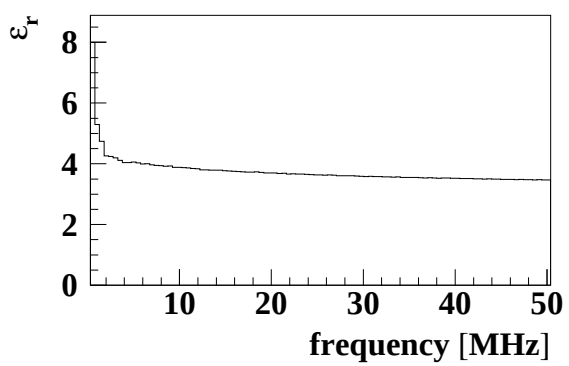

FIG. 12: Relative dielectric constant as a function of frequency.

polyimide its value can range typically from 3.2 to 3.5, with its nominal value given to be 3.2.[28]

The general layout of the stripline has been described in Section III B. The geometry used for the solution of Laplace's equation assumes that the conductive strips are separated vertically by a 50 μm thick layer of polyimide. A 50 μm thick outer polyimide layer is attached to the stripline with an adhesive. For simplicity, the adhesive is assumed to fill the lateral gap between the conductive strips with a thickness that is the same as the strip thickness (see Fig. 13).

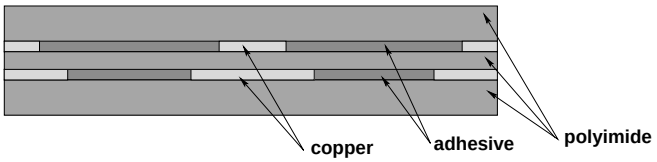

FIG. 13: Schematic geometry layout for the numerical treatment of Laplace's equation.

The following parameters have been varied: the widths and thicknesses of the signal and ground strips, and the relative dielectric constant of polyimide and the adhesive material [g]. In addition, the effects of possible misalignment between the signal and ground strips have been studied.

For each possible geometry Laplace's equation has to be solved twice, once for the case that the copper conductors are surrounded by vacuum and once for the case with polyimide and adhesive material present. The results yield two capacitances, C_v and C_ϵ respectively. The characteristic impedance can then be determined from:

$$Z_o = \frac{1}{c^2\sqrt{C_v C_\epsilon}} \ . \tag{A8}$$

	w_s (μm)	w_g (μm)	t (μm)	ϵ_p	ϵ_a	C_v (pF/m)	C_ϵ (pF/m)	Z_o (Ω)
a	200	360	34	3.2	4.0	51.4	172.5	35.4
b	200	360	34	3.4	4.0	51.4	182.4	34.4
c	200	360	34	3.2	4.4	51.4	174.1	35.4
d	200	360	30	3.2	4.0	51.0	171.8	35.6
e	190	360	34	3.2	4.0	49.7	167.6	36.5
f	180	360	34	3.2	4.0	48.3	162.4	37.6
g	180	315	34	3.2	4.0	47.2	158.8	38.5
h	220	385	34	3.2	4.0	55.0	171.8	34.3
i	200 →	360	34	3.2	4.0	51.2	172.1	35.5

TABLE II: The signal and ground strip widths and the strip thickness are labeled w_s, w_g, and t. ϵ_p and ϵ_a are the relative dielectric constants for polyimide and adhesive. Values of C_v, C_ϵ and Z_o are based on the numerical solution of Laplace's equation for various stripline geometries. Case **a** represents the nominal geometry. In case **i**, the arrow implies that there is a misalignment of 20 μm between the signal trace and the ground trace.

Table II lists the results of the calculations for various strip sizes and dielectric constants. It can be seen that the expected variations do not impact the performance of the vacuum cable significantly. The values of the impedance caused by the different variations of the geometry and material properties have a spread of approximately 4 Ω, which is in agreement with the width of the distribution of measured vacuum cable impedances.

In the high frequency approximation, the inductance is

$$L = 1/(c^2 C_v) \ . \tag{A9}$$

The resistance per unit length can be calculated as the resistivity of copper (1.72 $\mu\Omega$ cm) divided by the geometric cross section of the stripline conductors. The skin effect has to be taken into account in this calculation. For simplicity, we have assumed that the signal strip is fully penetrated when the skin depth δ is larger than half the thickness of the signal strip. For δ smaller than half the thickness of the signal strip, a band of thickness δ along the outer cross section of the signal strip is assumed to be homogeneously penetrated. The penetration depth of the ground strip is assumed to drop off exponentially, starting from the side of the ground strip that faces the signal strip. With these assumptions, the magnitude of the propagation constant can be calculated as

$$|\gamma|^2 = \gamma^* \gamma \ , \tag{A10}$$

with

$$\gamma = \sqrt{(R + i\omega L)(i\omega C)} \ . \tag{A11}$$

[g] No specific value is given in the data sheets for the adhesive alone, but specifications for dielectrics that give an average dielectric constant for polyimide and adhesive indicate that the dielectric constant of the adhesive alone is larger than that of the polyimide.

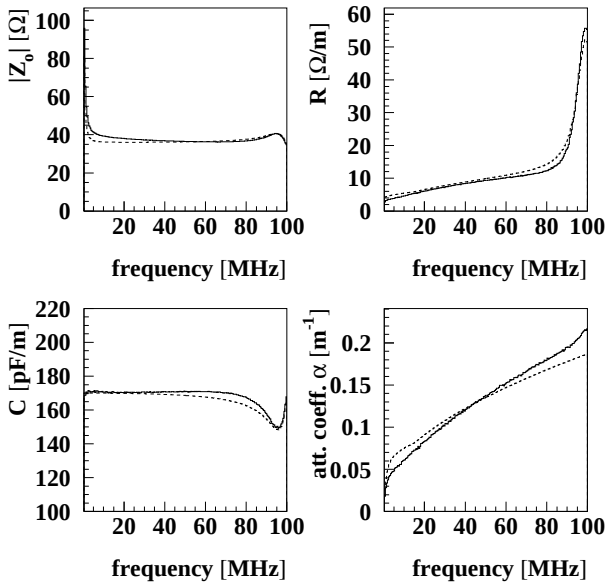

FIG. 14: Comparison of Z_o, R, C and α as determined from measurement (solid line) with the theoretical prediction of case **a** of Table II (dotted line).

The conductance G is very small compared to ωC and can be neglected in this case. The impedances for open and short circuit termination now become

$$Z_{oc} = Z_o \cdot \coth(\gamma l_{oc}) \ , \tag{A12}$$

$$Z_{sc} = Z_o \cdot \tanh(\gamma l_{sc}) \ , \tag{A13}$$

where l_{oc} and l_{sc} are the electrical lengths of the stripline with open circuit and short circuit termination.

It is now possible to calculate all the other stripline parameters as a function of frequency. Figure 14 shows a comparison of the measured values (solid line) of Z_o, R, C and α with the theoretical prediction for the vacuum cable (dashed line), given by case **a** of Table II. This comparison extends up to 100 MHz. The quarter wavelength range for the cable is reached at that point, resulting in a peak of the distributions due to a small difference in the electrical lengths of the measurements with open circuit and short circuit termination. In this case this difference has been modeled with a length of 40.2 cm for the open circuit case and 41.4 cm for the short circuit case.

The results of the theoretical calculations are in good agreement with the measurements. The differences between the calculation and the data can be attributed to the high frequency TEM mode approximation, the simplified treatment of the skin effect and the uncertainty in dielectric parameters. It should be noted at this point that the connectors of the vacuum cable cannot be easily modeled, but do have an impact on the performance. Nevertheless, the level of agreement is more than adequate to evaluate the effects of various stripline parameters.

[1] ATLAS Collaboration, *ATLAS Calorimeter Performance Technical Design Report*, CERN document **CERN/LHCC 96-040**, 1997.

[2] ATLAS Collaboration, *Liquid Argon Calorimeter Technical Design Report*, CERN document **CERN/LHCC 96-041**, 1996.

[3] ATLAS Electromagnetic Liquid Argon Calorimeter Group, *Construction of the ATLAS electromagnetic calorimeter barrel*, to be published in *Nucl. Instrum. Methods* A (2004).

[4] M. Fincke-Keeler, R.K. Keeler and M. Lefebvre, *Performance Requirement of the Signal Feedthrough Vacuum Cables*, ATLAS internal document **ATL-AE-EN-0002**, 1999.

[5] D. Axen et al., *Performance of the Signal Vacuum Cables of the Liquid Argon Calorimeter Endcap Cryostat Signal Feedthroughs*, ATLAS internal document **ATL-AE-EN-0015**, 2003.

[6] ASME Boiler and Pressure Vessel Committee, Subcommittee on Pressure Vessels, *ASME Boiler and Pressure Vessel Code, Section VIII, Rules for Construction of Pressure Vessels*, 1992 Edition, American Society of Mechanical Engineers, New York.

[7] Glasseal Products, Inc., 485 Oberlin Ave., Lakewood, NJ 08702.

[8] G. Macé, P. Pailler, and J. Sonderiker, *Load cases for cryostats and feedthroughs*, ATLAS internal document **ATL-AE-ES-0009**, 1999.

[9] T. Hodges and M. Lefebvre, *Finite element analysis and the ATLAS liquid argon calorimeter signal feedthrough assembly*, ATLAS internal document **ATL-AE-EA-0005**, 2001.

[10] J.T. Koehler, *US ATLAS Formed Metal Feed-Through Bellows Assemblies*, BNL document **BNL-ATLAS-3213-101**, 1999.

[11] B. Szeless, *Report on the Production Readiness Review for the ATLAS LAr Signal Feed Throughs*, ATLAS internal document **ATC-RA-ER-0005**, CERN Document **EB-99-001**, 1999.

[12] Expansion Joint Manufacturers Association, Inc., *Standards of the Expansion Joint Manufacturers Association, Inc.*, Ed. 7, 1998, Tarrytown, New York.

[13] Syndicat National de la Chaudronnerie, de la Tolerie et de la Tuyauterie Industrielle, *CODAP French Code for Construction of Unfired Pressure Vessels*, Edition 1995, Paris.

[14] American BOA, Inc., 1420 Redi Road, Cumming, GA 30040.

[15] Edited by: Director General, *CERN Code de Sécurité/Safety Code D2, Rev. 2, Pressure Equipment*.

[16] S. Kane et al., *unpublished*.

[17] C. Cerna et al., *Cabling of the ATLAS liquid argon calorimeters*, ATLAS internal document **ATL-A-EN-0001**, 2004.

[18] M. Fincke-Keeler, M. Lefebvre, and P. Poffenberger, *Cabling of the Endcap Signal Feedthroughs*, ATLAS internal document **ATL-AE-AN-0002**, 2000.

[19] FCI Electronics, 5700 Warland Drive, Cypress, CA 90630.

[20] W. Bonivento et al., Nucl. Instr. and Meth. **A451**, 492 (2000).

[21] Axon' Cables SA, Route de Chalons en Champagne, F-51210 Montmirail.

[22] M. Fincke-Keeler amd M. Lefebvre, *A Proposal for a Low Voltage Vacuum Cable Design for the HEC Feedthroughs in the ATLAS Endcap Cryostat*, ATLAS internal document **HEC 068**, 1998.

[23] J. Farrell, R. Hackenburg, and D. Makowiecki, *Description of the LAr Barrel Calorimeter Signal Feedthrough Filter Box*, ATLAS internal document **ATL-AB-CD-0001**, 2002.

[24] Critedes Technical Associates, 7700 River Road, One Marine Plaza - Suite 207, North Bergen, NJ 07047.

[25] R. Hackenburg, *Operator's Manual for the FT2001 ATLAS Barrel Signal Feedthrough Automated Electrical Tester*, ATLAS internal document **ATL-AB-TP-0001**, 2002.

[26] For access to this database, see http://atlas.web.cern.ch/Atlas/GROUPS/LIQARGON/Data_Bases/index.html

[27] T.C. Edwards, *Foundations for Microstrip Circuit Design*, John Wiley & Sons, 1981.

[28] See data sheets on: http://www.dupont.com/kapton.